Vulnerability of a partially flooded PWR reactor cavity to a steam explosion

Leon Cizelj, Boštjan Končar, Matjaž Leskovar
"Jožef Stefan" Institute
Jamova 39, SI 1000 Ljubljana, Slovenia

Corresponding Author: Prof. Dr. Leon Cizelj
phone + 386 1 5885 215; fax + 386 1 5885 377; e-mail: Leon.Cizelj@ijs.si

Keywords

Steam explosion, reactor cavity, vulnerability

Abstract

When the hot molten core comes into contact with the water in the reactor cavity a steam explosion may occur. A steam explosion is a fuel coolant interaction process where the heat transfer from the melt to water is so intense and rapid that the timescale for heat transfer is shorter than the timescale for pressure relief. This can lead to the formation of shock waves and later, during the expansion of the water vapour, to production of missiles that may endanger surrounding structures.

The purpose of the performed analysis is to provide an estimation of the expected pressure loadings on the typical PWR cavity structures during a steam explosion, and to make an assessment of the vulnerabilities of the typical PWR cavity structures to steam explosions. To achieve this, the fit-for-purpose steam explosion model is proposed, followed by comprehensive and reasonably conservative analyses of two typical ex-vessel steam explosion cases differing in the steam explosion energy conversion ratio. In particular, the vulnerability of the surrounding reinforced concrete walls to damage has been sought in both cases.

1 Introduction

In some hypothetical severe accident scenarios it is assumed that the pressure vessel is cooled from the outside by water, which resides in the reactor cavity. Such an approach is known as the "wet cavity". It has been nevertheless argued that outside cooling may not be sufficient and that it is possible that the vessel will not be able to contain the already molten core (Esmaili and Khatib-Rahbar, 2005; Asmolov et al., 2001). There exists also the possibility that the reactor vessel will fail even before the water level in the reactor cavity raises sufficiently to submerge the lower part of the reactor vessel (Leskovar et al., 2005a).

When the hot molten core exits the vessel, it will come into contact with the water in the reactor cavity. Such a contact might lead to a steam explosion. A steam explosion is a fuel coolant interaction process where the heat transfer from the melt to water is so intense and rapid that the timescale for heat transfer is shorter than the timescale for pressure relief (Berthoud, 2000). This can lead to the formation of shock waves and later, during the expansion of the water vapour, to production of missiles that may endanger surrounding structures.

A steam explosion is a complex, highly nonlinear, coupled multi-component, multi-phase, multi-space-scale and multi-time-scale phenomenon. Consequently, modelling of steam explosions is a difficult task and the uncertainties of reactor simulations performed with steam explosion codes based on modelling fundamental steam explosion processes are still large (Magallon et al., 2005). The assessment of the reactor cavity vulnerability to an ex-vessel steam explosion therefore requires a parametric approach capturing the uncertainties of steam explosion understanding and modelling.

The main goal of the present study is to estimate the dynamic pressure loads and stresses to predict the vulnerability of the cavity structures. To achieve this, the fit-for-purpose steam explosion model, which can be straightforwardly implemented in a general purpose Computational Fluid Dynamics (CFD) code, is proposed. Analyses of two typical ex-vessel steam explosion cases differing in the steam explosion energy conversion ratio follow. Both cases assume that the melt is poured in the central region just below the pressure vessel. Cases with melt poured sideways are discussed elsewhere (Leskovar et al., 2005b).

The steam explosion was modelled as an expanding high-pressure premixture of dispersed molten fuel, liquid water and water vapour in the partially flooded reactor cavity. A similar, although less sophisticated approach was used also in the steam explosion study performed by Almstroem et al. (1999). The expansion of the high-pressure premixture in the reactor cavity partially flooded with coolant water was simulated with the CFD code CFX-5.7.1 (ANSYS-CFX Development Team, 2004) and the stresses in the cavity structures were simulated by the stress analysis code ABAQUS/Explicit (Hibbit et al., 2002).

2 MODEL

2.1 Steam Explosion Phenomenon

Steam explosions are a subclass of the so-called fuel coolant interactions (FCI) in safety studies of nuclear reactors. Based on the phenomena occurring during a steam explosion it can be divided into four consecutive phases: the premixing phase, the triggering phase, the propagation phase and the expansion phase (see Figure 1).

(Insert Figure 1)

Premixing phase

In the premixing phase the molten jet breaks up (Burger et al., 1995) and a coarsely mixed region of molten corium and coolant water is formed. A vapour film separates the melt and water, so the heat transfer between the melt and water is relatively low. The premixing phase is characterized by a steam production rate at a timescale of the same order as the timescale of the melt pouring rate. It results in a slow pressurization of the system, or even not, if condensation is able to balance vaporization. The system can remain in this metastable state till the melt is quenched or, if the conditions are appropriate, till a steam explosion is triggered. The timescale of the premixing process is in the range of seconds, and the length scale of the melt particles is in the range of centimetres.

Triggering phase

In the triggering phase the steam explosion is triggered. The triggering event is a disturbance, which destabilizes the vapour film around a melt particle allowing liquid-liquid contact, which leads to locally enhanced heat transfer, pressurization and local fine fragmentation. Many reasons can cause vapour film destabilization, including pressure pulses resulting from different impacts (in experiments interactions are often triggered when the melt reaches the bottom of the tank), transition from film boiling to nucleate boiling, and water entrapment at melt-structure contact.

Propagation phase

During the propagation phase, an escalation process takes place resulting from the coupling between pressure wave propagation, fine fragmentation, and heat transfer after the triggering event. The pressurization induced by the triggering event destabilizes the surrounding vapour films, leading to the fine fragmentation of the surrounding melt. Early in the process, fine fragmentation results from local liquid-liquid contacts after the vapour film destabilization.

Locally, some coolant is rapidly heated and pressurized, and this causes some fine fragmentation of the surrounding melt. This type of fragmentation is often called thermal fragmentation. Later, when the pressure is already high, the fine fragmentation is believed to be of a hydrodynamic nature owing to the relative motion between the melt and the coolant induced by their different densities and compressibilities. The fine fragmentation propagates at a velocity, which depends on the conditions in the premixing region. It can be governed by timescales corresponding to the propagation of disturbances in the premixing region, resulting in sequential ignition of the mixture. Typical velocities in this case are in the order of some tens of meters per second. In this case, the pressurization of the system is relatively limited, slow and uniform, without generation of shock waves. But the fine fragmentation can escalate also up to reaching supersonic velocities in the pre-mixture and quasi steady state propagation. Depending on the conditions, the pre-mixture can "burn" more or less completely before the system can expand, thus creating a zone of high pressure. During the propagation phase the thermal energy of the melt is converted into thermal energy of the coolant. The timescale of the explosion propagation process is in the range of milliseconds, and the length scale of the fine fragmented particles is in the range of hundreds of micrometers.

Expansion phase

During the expansion phase the thermal energy of the coolant is converted into mechanical energy. The expansion of the high-pressure mixture against the inertial constraints imposed by the surroundings determines the damage potential of the steam explosion. The damage might be caused through pressure shock waves at the beginning of the process and afterwards through the kinetic energy transmitted to the surrounding cavity structures. If the localized high pressures are quickly relieved, then they may not damage the surrounding structures, but the kinetic energy transmitted to the materials around the interaction zone may be the damaging agent.

A comprehensive description of the steam explosion phenomenon is provided by Berthoud (2000) and Turland and Dobson (1996).

2.2 Steam Explosion Model

To be able to treat the steam explosion with a general purpose CFD code, an appropriate fit-for-purpose analytical model of the steam explosion was developed. For the specialized steam explosion CFD codes it is customary to model steam explosion on the micro-scale using fundamental averaged multiphase flow conservation equations (Berthoud, 2000; Turland and

Dobson, 1996; Leskovar and Mavko, 2000). In contrast, the approach proposed in this paper models the steam explosion in a reasonably simplified fashion as an expanding high-pressure premixture of dispersed molten fuel, liquid water and water vapour. A similar approach was also used in the steam explosion study performed by Almstroem et al. (1999), where the steam explosion was treated less sophisticated as an expanding high-pressure vapour bubble.

In general, the proposed steam explosion model is based on the Hicks-Menzies thermodynamic approach (Berthoud, 2000) taking into account the microinteraction zone concept (Yuen and Theofanous, 1995). According to the microinteraction zone concept only a part of the coolant thermally participates in the explosion - only the coolant, which is in the surroundings of the melt particles. In Figure 2 the steam explosion model is schematically presented. The corium phase is denoted with the red/dark grey colour and the superscript *cor*, the vapour phase with the light blue/light grey colour and the superscript *vap* and the liquid water phase with the dark blue/black colour and the superscript *wat*. It was assumed that all phases share the same velocity field and the same pressure. In the presented control volume each phase is described with the phase volume fraction α, volume V, density ρ and temperature T. The microinteraction zone is denoted with the dotted blue/black colour and the superscript MI.

(Insert Figure 2)

In the model it was assumed that the heat transfer from the molten fuel to the coolant was completed during the first three steam explosion phases and that during the expansion phase the generated vapour, which is at high pressure, expands adiabatically. The performed work $A_{2\to 3}$ during the presumed adiabatic expansion can be calculated as

$$A_{2\to 3} = \int_{V_2^{vap}}^{V_3^{vap}} p dV = -\frac{p_2 \left(V_2^{vap}\right)^{\kappa}}{\kappa - 1} \frac{1}{V^{\kappa-1}} \Bigg|_{V_2^{vap}}^{V_3^{vap}} = \frac{p_2 V_2^{vap}}{\kappa - 1} \left(1 - \left(\frac{p_3}{p_2}\right)^{\frac{\kappa-1}{\kappa}}\right), \qquad (1)$$

where p_2 and p_3 are the pressures at the start and at the end of the expansion phase, and κ is the ratio between the vapour specific heats at constant pressure and at constant volume.

An important parameter of the steam explosion is the steam explosion energy conversion ratio, which is quantified also in steam explosion experiments and reflects how much internal energy of the melt is transformed into the mechanical energy of the explosion (Berthoud, 2000). In the proposed model the steam explosion energy conversion ratio η was used as the basis for the calculation of all other steam explosion parameters. When the conditions during the premixing phase are selected, the pressure at the start of the expansion phase p_2 can be calculated by iteratively solving the equation

$$p_2 = \eta \frac{(\kappa - 1)\rho_1^{cor} \alpha_1^{cor} c^{cor} \left(T_1^{cor} - T_1^{sat}\right)}{\alpha_2^{vap} \left(1 - \left(\frac{p_3}{p_2}\right)^{\frac{\kappa-1}{\kappa}}\right)}, \tag{2}$$

where p_3 is the containment pressure, c^{cor} is the corium specific heat and T_1^{sat} is the water saturation temperature at containment pressure. The volume fraction of the microinteraction zone α^{MI}, which determines the vapour volume fraction at the beginning of the expansion phase $\alpha_2^{vap} = \alpha^{MI} + \alpha_1^{vap}$, was chosen in such a manner that the pressure at the start of the expansion phase p_2 was maximized, considering the physical feasibility of the process. Due to the assumption of the adiabatic vapour expansion, the density of the premixture during the expansion process $\rho_{2\to3}^{mix}$ can be calculated solely as a function of pressure

$$\rho_{2\to3}^{mix}(p) = \frac{\rho_2^{mix}}{\left(1 - \alpha_2^{vap}\right) + \frac{\alpha_2^{vap}\rho_2^{vap}}{\rho_{2\to3}^{vap}(p)}} = \frac{\rho_2^{mix}}{1 + \alpha_2^{vap}\left(\left(\frac{p_2}{p}\right)^{\frac{1}{\kappa}} - 1\right)}, \tag{3}$$

where ρ_2^{mix} is the premixture density at the start of the expansion phase and $\rho_{2\to3}^{vap}$ the vapour density during the expansion phase.

With the developed analytical steam explosion model the initial conditions at the start of the expansion phase are determined, whereas the expansion phase itself has to be simulated with the CFD code taking into account the derived equation of state for the premixture (eq. 3). The

deficiency of the proposed parametrical steam explosion model is that the calculated premixture high-pressure p_2 at the start of the expansion phase depends on the selected premixing conditions, since an identical steam explosion energy conversion ratio η can be obtained with different combinations of the premixture vapour fraction α_2^{vap} and premixture pressure p_2 (lower α_2^{vap} results in higher p_2). As the destructive consequences of an explosion depend mainly on the pressure impulse of the explosion (i.e. integral of pressure over time), this characteristic of the model does not present a serious weakness for our study. Namely, according to the premixture equation of state (eq. 3) also the duration of the pressure impulse is shorter at lower α_2^{vap}, and so the effect of the increased pressure peak is mainly compensated. In any case, due to the large uncertainties in understanding and modelling of steam explosions, a sufficient degree of conservatism has to be introduced in whichever approach taken. A detailed description of the developed steam explosion model is provided in (Leskovar et al., 2005a).

2.3 Computational Fluid Dynamics Model

The multiphase flow during the steam explosion expansion phase consists of three phases – the premixture phase (mixture of dispersed molten fuel, liquid water and water vapour), the liquid water phase and the air phase – and was simulated by the CFX-5.7.1 code. To simulate the pressure waves, all three fluids were treated as compressible and were modelled by the homogeneous Eulerian model, which assumes that all phases share a common velocity field. The effect of turbulence was taken into account with the k-ε turbulence model. The energy equation was not solved since the heat transfer during the steam explosion was taken into account already at the initial conditions, and cooling of the vapour in the premixture during the expansion process was taken into account already within the adiabatic premixture equation of state (eq. 3). The equation of state for water was determined using the standard water steam tables and air was treated as an ideal gas. For other material properties the default values as provided by the CFX-5.7.1 code were used.

Since the CFD calculation did not converge on a relatively coarse numerical grid appropriate from the physical point of view, and since the required CPU times for the three-dimensional (3D) calculation on the refined grid would be exceedingly long, the calculations were performed using the two-dimensional (2D) axially symmetric geometry model. The 2D axially symmetric model is limited to the treatment of axially symmetric phenomena in the cylindrical part of the reactor cavity directly below the reactor vessel and around it. To assure that the simulation results with the 2D model would be qualitatively and quantitatively valid also for the real 3D geometry of the reactor cavity, the 2D geometry and the initial conditions had to be appropriately selected. The geometry and mesh of the CFD model is presented together with the structural model on Figure 3. The detailed description of the CFD model is provided in (Leskovar et al., 2005a).

(Insert Figure 3)

2.4 Structural Model

Based on the geometry of the problem, it is deemed sufficient to develop an axially symmetric model of the cylindrical part of the reactor cavity. The model properly accounts for the fact that the cavity walls are to a significant height embedded by the foundation of other containment structures.

All the walls potentially affected by the steam explosion in the typical PWR reactor cavity are made of heavily reinforced concrete. The minimum required compressive strength of the concrete was assumed to be 30 MPa and the minimum required yield strength of the reinforcement steel was assumed to be 400 MPa.

The material model used in the simulations is simplified to a significant extent and is aimed at detection of significant damage rather than to give an accurate account on the deformation history of the complex and non-homogeneous reinforced concrete. A homogeneous and essentially elastic response was therefore assumed both in tension and compression. The main “effective” parameters of the model assuming about 10 vol.% of reinforcement steel were: density of 2945 kg/m3, Young’s modulus of 45 GPa and Poisson’s ratio of 0.174.

The yield strength of 250 MPa was arbitrarily assumed beyond the loading regime experienced in the simulation. The main purpose of that was to enable the use of approximate

damage models, which are built in the ABAQUS/Explicit code. The damage was assumed to occur instantly with (tensile or compressive) hydrostatic pressure exceeding 50 MPa.

Loads include dead weight and pressure histories obtained from the CFX simulation results. The variations of pressures in time and space were included in the ABAQUS/Explicit code using the FORTRAN subroutine VDLOAD. Linear interpolation between data points was used both in space and in time.

The finite element model of the cavity walls is presented together with the geometry of the CFD model in Figure 3. Further details are available in (Leskovar et al., 2005a).

3 Numerical Example

3.1 Input

Due to the variegated spectrum of ex-vessel steam explosion scenarios and the large uncertainty in steam explosion understanding and modelling, a comprehensive ex-vessel steam explosion sensitivity analysis has been undertaken and is reported elsewhere (Leskovar et al., 2005a). In this section, two typical ex-vessel steam explosion cases following a reasonable conservative ex-vessel central melt pour scenario at a depressurised primary system are presented in some detail. Both simulated cases, differing in the presumed steam explosion energy conversion ratio, are based on the following common assumptions:

- The reactor cavity is partially flooded. The water level in the cavity is 3 m.
- The premixture is located in the middle of the cavity in a cylindrical region with diameter of 1.6 m and height of 3 m.
- The premixture is homogenous with the following volume fractions of the constituents: corium 0.1, water vapour 0.1 and liquid water 0.8.
- The corium temperature is 2800 K. It was assumed that there is no Zr oxidation.
- The cavity water temperature is 343 K and the containment pressure is 1.5 bar.
- At the start of the simulated steam explosion expansion phase the whole premixture is homogenously pressurized.

At small-scale experiments with prototypic corium materials (UO_2+ZrO_2, …) the maximum obtained steam explosion energy conversion ratios are about 0.5% and the maximum measured peak pressures are about 200 bar (Berthoud, 2000; Magallon et al., 2000; Corradini, 1991). The effect of scaling was studied in the Winfrith scaling experiments performed with 0.5 kg and 24 kg UO_2-Mo thermite sources at different water subcooling (Berthoud, 2000). They showed that

the steam explosion energy conversion ratio does not depend on the scale, but it is difficult to extrapolate this conclusion to reactor-scale systems, where the involved melt masses are more than two orders of magnitude larger. There are physical reasons that favour an increase in the steam explosion efficiency with scale, like the potentially increased times for heat transfer due to the more constrained system, but there are also reasonable counter arguments, like that it is difficult to get a "good" large size premixture, because more melt implies more vapour production during premixing and consequently less liquid water to interact with the melt.

Due to these scaling uncertainties and to find out the influence of the steam explosion energy conversion ratio on the simulation results, the simulations were performed with two different steam explosion energy conversion ratios:

- Case 1: The steam explosion energy conversion ratio is 1 %, resulting (according to the proposed steam explosion model) in the premixture initial pressure of 400 bar.
- Case 2: The steam explosion energy conversion ratio is 10 %, resulting in the premixture initial pressure of 2500 bar.

Both selected steam explosion energy conversion ratios and the resulting premixture initial pressures are conservative according to the performed small-scale experiments with prototypic corium materials. This selection of the steam explosion energy conversion ratios seems to be reasonable also if we consider steam explosion experiments with various simulant materials, where the steam explosion energy conversion ratios and the pressures are much higher than at experiments with prototypic corium materials (Huhtiniemi et al., 1999; Corradini, 1991).

3.2 Results

3.2.1 Case 1: Conversion ratio 1 %, Pressure 400 bar

To get a qualitative and quantitative picture of the multiphase flow during the steam explosion in the reactor cavity the basic results of the CFD simulation are depicted in Figure 4 and Animation 1. They include the time development of the pressure field, the velocity field and the volume fractions of the mixture and water. It can be seen that the initially sharp interfaces

between the mixture, water and air phases spread during the transient due to numerical diffusion, which is characteristic for finite difference numerical methods (Leskovar, 2000). Due to the nature of the modelling approach adopted this interface spreading has no significant influence on the main simulation results and on the conclusions of the performed study.

(Insert Figure 4 and Animation 1)

The area indicating the origin of the steam explosion at the initial time (t = 0 seconds) is shown with the red/light grey coloured high-pressure region and with the red/light grey coloured mixture region embedded below the centre of the reactor vessel. The velocities are at this stage still zero in the entire computational area. The high-pressure in the premixing zone in the central part of the cavity causes the expansion of the mixture, which pushes the water and air through the annulus around the reactor vessel. After 0.0125 s the mixture is practically completely surrounded with water, as the water can be pushed only upwards (no openings in the side walls of the cylindrical part of the cavity are modelled). At later times, when the pressure is already low, the water flows back into the lower part of the cavity and a big vortex is formed. The maximum fluid velocities are above 300 m/s and are reached at the outlet of the annulus at about 0.05 seconds.

Figure 5 depicts the pressure histories at selected locations, which are of importance for the assessment of the vulnerability of cavity structures. These locations are denoted in Figure 3 with L1 to L4. It can be seen that the pressure is the highest in the first milliseconds of the transient during the premixture high-pressure relief when also pressure shocks propagate to the walls. The pressure loads on the cavity walls at later times, which are caused by the impact of the fluids with high velocity, are much lower.

(Insert Figure 5)

The response of the cavity walls to the dynamic pressure loading described above is depicted in Figures 6 and 7 and Animation 2. The Mises stresses in the walls of the cylindrical part of the reactor cavity are plotted as a function of time with snapshots at 1, 2, 3 and 5 ms. The stresses are caused by the walls pressure loading during the premixture high-pressure relief with maxima occurring within the first 3 ms.

The damage criteria have not been exceeded in this simulation. It is therefore judged that the cavity walls at the considered steam explosion scenario (400 bar) would not be damaged. Further details are available in (Leskovar et al., 2005a).

(Insert Figure 6 and Figure 7 and Animation 2)

3.2.2 Case 2: Conversion ratio 10 %, Pressure 2500 bar

Since the simulation of Case 1 showed that the pressure loads on the cavity walls are the highest during the premixture high-pressure relief when also pressure shocks propagate to the walls, we focused in Case 2 only on the first milliseconds of the transient.

Figure 8 and Animation 3 depict the pressure field, the common velocity field and the mixture and water volume fractions during the premixture high-pressure relief. It can be seen how the pressure wave originating from the steam explosion zone in the central part of the reactor cavity (t = 0 s) propagates horizontally to the cavity wall (t = 0 s -0.002 s), where it is reflected back in the central region of the cavity (t = 0.002 s - 0.006 s) causing the pressure to be the highest again on the left side of the computational area. At the same time the high pressure is relieved in vertical direction in the air phase and a rare-fraction wave propagates to the bottom of the cavity. During the premixture high-pressure relief the mixture already starts to expand mainly upward. Already after 6 ms of the transient the highest velocities of more than 450 m/s are reached at the mixture front. At that time the mixture is pushed through the narrow region forming between the reactor vessel and the rising water phase.

(Figure 8 and Animation 3)

Figure 9 shows the pressure histories at locations L1 to L4 (see Figure 3) within the first 8 ms of the transient. Since during that short time the pressure shock waves did not reach the locations L3 and L4 yet, the pressure at these locations is still equal to the containment pressure of 1.5 bar and therefore too low to be resolved on the diagram. Rather high-pressure peaks of about 1200 bar propagate to the walls in the times of the order of 1 ms. Also, the duration of the pressure pulse is in the order of ms.

(Insert Figure 9)

The response of the cavity walls to the dynamic pressure loading described above is depicted in Figure 10, Figure 11 and Animation 4. The Mises stresses in the walls of the cylindrical part of the reactor cavity are plotted as a function of time with snapshots at 1, 2, 3 and 5 ms. The stresses are caused by the walls pressure loading during the premixture high-pressure relief with maxima occurring within the first 3 ms.

The damage criteria have been slightly exceeded at certain localized spots. These spots are denoted with black colour in Figure 10, Figure 11 and Animation 4. The damage develops in both in tensile and compressive regimes and reaches full extent within first 3 to 5 ms of the simulation. This is consistent with the time scale of the wall loading by the pressure impulse. It is judged that there is a potential for minor to medium localized damage. It is estimated that the collapse of the walls is not probable.

(Insert Figure 10, Figure 11 and Animation 4)

4 Conclusions

The purpose of the performed analysis is to provide an estimation of the expected pressure loadings on the typical PWR cavity structures during an ex-vessel steam explosion, and to make an assessment of the vulnerabilities of the typical PWR cavity structures to steam explosions. To be able to perform the analysis with a general purpose CFD code, the fit-for-purpose steam explosion model is proposed. A comprehensive and reasonably conservative analysis was performed. In particular, the vulnerability of the surrounding reinforced concrete walls to damage has been sought.

Two typical ex-vessel steam explosion cases with energy conversion ratio 1 % and 10 % resulting in premixture pressures of 400 bar and 2500 bar were analysed. The multiphase flow during the steam explosion expansion phase was simulated by the CFX-5.7.1 code. The calculated dynamic pressure loads on the cavity walls were taken as the input for the ABAQUS/Explicit simulation of the stresses in the cavity walls. The response of the cavity walls to the dynamic pressure loads was compared against the pre-established damage criteria.

The CFD simulations showed that the pressure loads on the cavity walls are the highest during the premixture high-pressure relief, when also pressure shocks propagate to the walls. This process is completed within the first 3 to 5 ms. The pressure loads on the cavity walls at later times were caused by the impact of the high velocity fluid and did not pose any threat to the cavity walls.

The dynamic response of the cavity walls, simulated by ABAQUS/Explicit, showed no damage in the case of premixture pressure of 400 bar and some potential for minor to medium localized damage in the case of premixture pressure of 2500 bar. In both cases, it is estimated that the collapse of the cavity walls is not probable.

For a more detailed insight of the steam explosion phenomenon in the typical PWR cavity and its potential consequences, more refined models should be implemented or developed. This goes especially for the modelling of the steam explosion dynamics and the modelling of the

reinforced concrete and damage processes therein. Future analyses should also address the high-pressure melt ejection scenarios and the potential consequences of successive steam explosions.

5 Acknowledgments

This work was financially supported in part by the Ministry of Higher Education, Science and Technology (partly through the research program P2-0026 and partly through the research project J2-6565). The Jožef Stefan Institute is a member of the Severe Accident Research Network of Excellence (SARNET) within the 6th EU Framework Programme.

6 References

ANSYS-CFX Development Team, 2004. CFX-5.7.1 Documentation, ANSYS Inc.

H. Almstroem, T. Sundel, W. Frid, A. Engelbrektson, 1999. Significance of Fluid-Structure Interaction Phenomena for Containment Response to Ex-Vessel Steam Explosions. Nuclear Engineering and Design 189, 405-422.

V. Asmolov, N.N. Ponomarev-Stepnoy, V. Strizhov, B.R. Sehgal, 2001. Challenges left in the area of in-vessel melt retention. Nuclear Engineering and Design 209, 87-96.

G. Berthoud, 2000. Vapour Explosions. Annu. Rev. Fluid Mech. 32, 573-611.

M. Burger, S.H. Cho, E.v. Berg, A. Schatz, 1995. Breakup of melt jets as pre-condition for premixing: Modeling and experimental verification. Nuclear Engineering and Design 155, 215-251.

M.L. Corradini, 1991. Vapor Explosions: A Review of Experiments for Accident Analysis. Nuclear Safety 32(3), 337-362.

H. Esmaili, M. Khatib-Rahbar, 2005. Analysis of likelihood of lower head failure and ex-vessel fuel coolant interaction energetics for AP1000. Nuclear Engineering and Design 235, 1583-1605.

Hibbit, Karlsson and Sorrensen Inc., 2002. ABAQUS/EXPLICIT 6.4-1, www.abaqus.com.

I. Huhtiniemi, D. Magallon, H. Hohmann, 1999. Results of Recent KROTOS FCI tests: Aluminia versus Corium Melts. Nuclear Engineering and Design 189, 379-389.

M. Leskovar, L. Cizelj, B. Končar, I. Parzer, B. Mavko, 2005a. Analysis of influence of steam explosion in flooded reactor cavity on cavity structures. Report IJS-DP-9103, Institut "Jožef Stefan", Ljubljana, Slovenia.

M. Leskovar, B. Končar, L. Cizelj, 2005b. Simulation of Ex-Vessel Steam Explosion with a General Purpose Computational Fluid Dynamic Code. Submitted to Strojniški vestnik.

M. Leskovar, B. Mavko, 2000. The influence of the Accuracy of the Numerical Methods on Steam-Explosion Premixing Phase Simulation Results. Journal of Mechanical Engineering 46, 607-621.

D. Magallon et al., 2005. Insight into the Results of International Programme SERENA on Fuel-Coolant Interaction. NURETH-11, Avignon, France, October 2-6, 2005.

D. Magallon et al., 2000. MFCI Project – Final Report. INV-MFCI(99)-P007, EUR 19567.

B.D. Turland, G.P. Dobson, 1996. Molten Fuel Coolant Interactions: A state-of-the-art report. EUR 16874 EN.

W.W. Yuen, T.G. Theofanous, 1995. The Prediction of 2D Thermal Detonations and Resulting Damage Potential. Nuclear Engineering and Design 155, 289-309.

LIST OF FIGURES

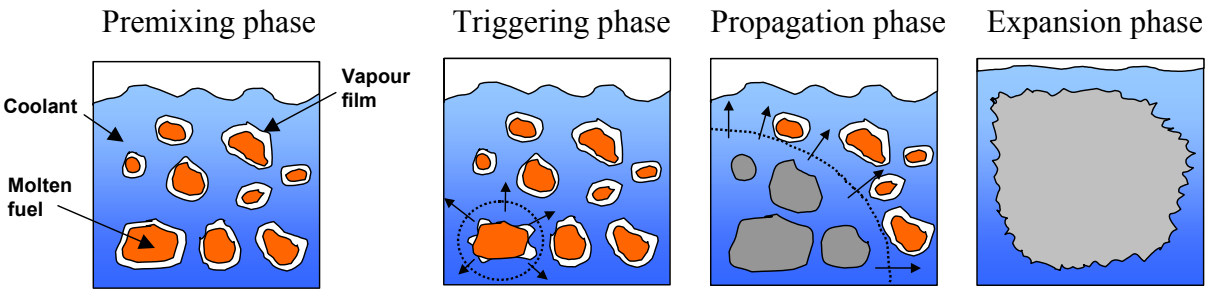

Figure 1 **Schematic presentation of the four consecutive phases of the steam explosion.**

a) Premixing phase (index 1)

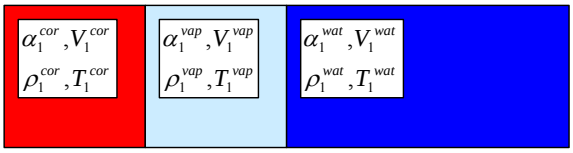

b) Triggering and Start of Propagation phase

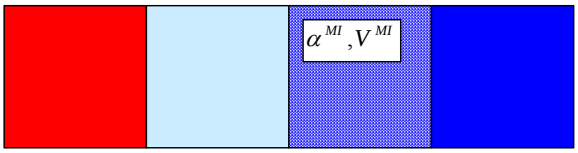

c) End of Propagation phase and Start of Expansion phase (index 2)

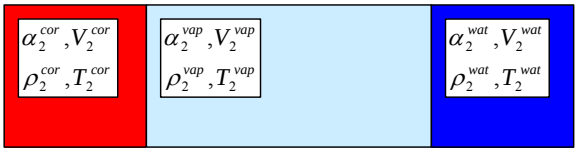

d) End of Expansion phase (index 3)

Figure 2 Schematic presentation of steam explosion model (red/dark grey – molten core, light blue/light grey – water vapour, dark blue/black – liquid water, dotted blue/black – liquid water in microinteraction zone).

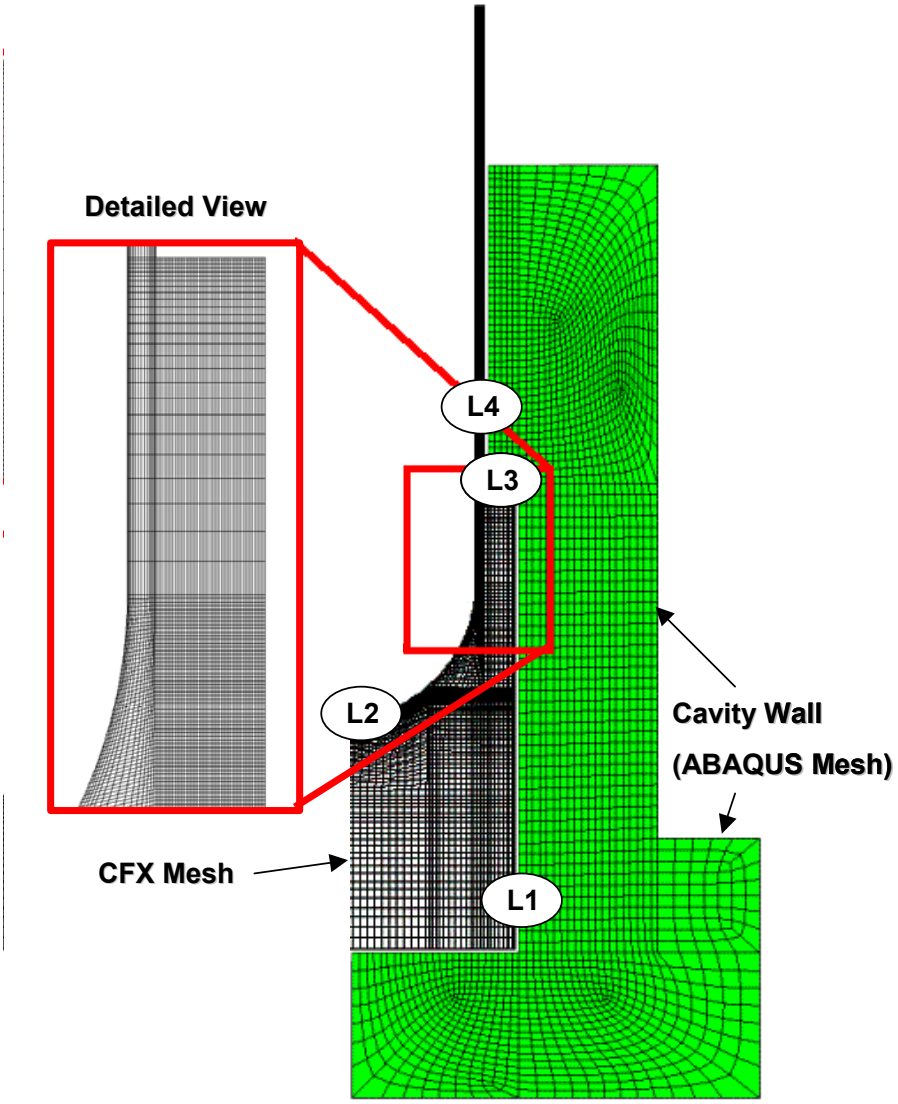

Figure 3 **Geometry and mesh of CFX computational fluid dynamics model of reactor cavity (black) and ABAQUS structural model of cavity wall (green/gray).**

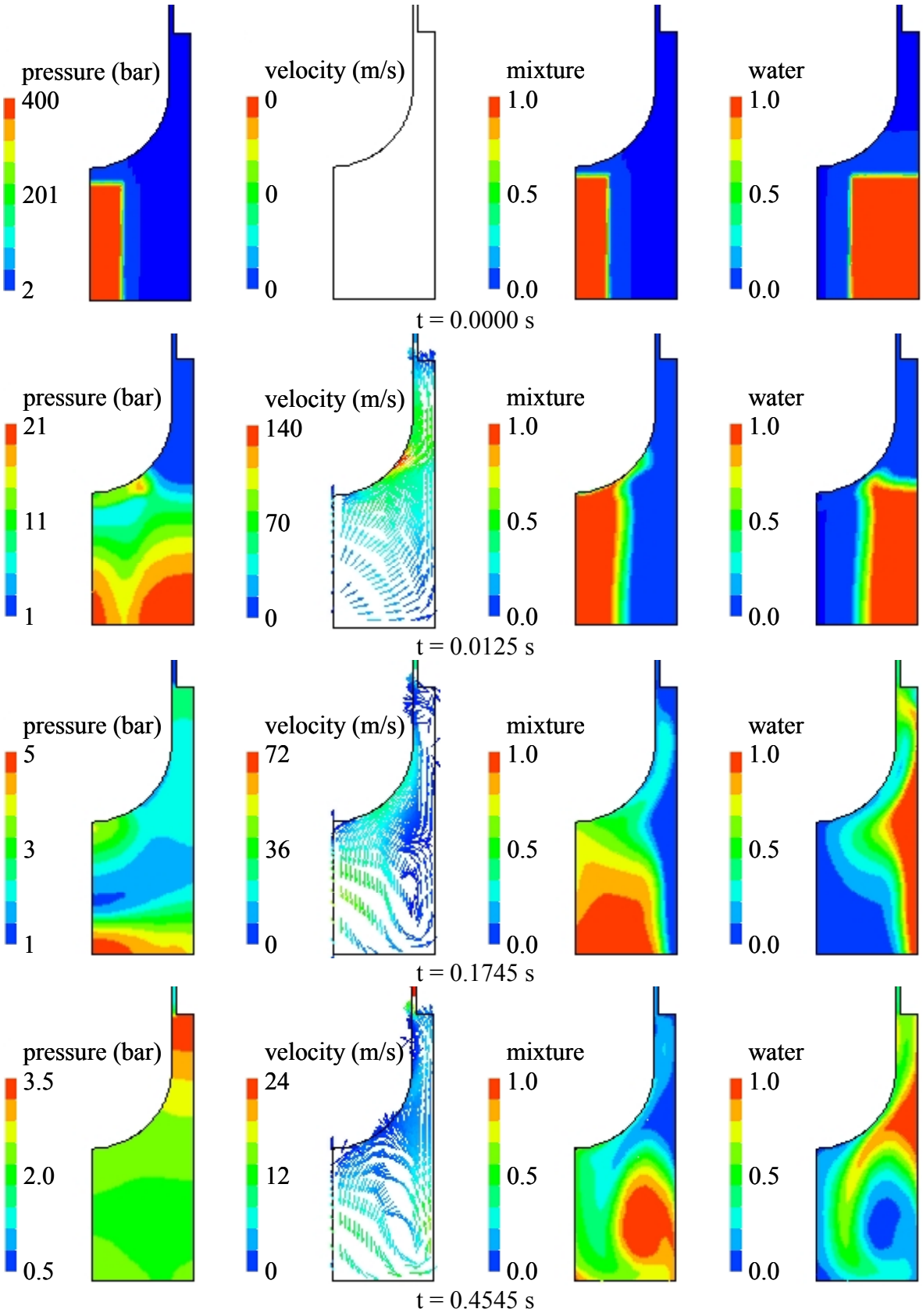

Figure 4 CFD Results for 400 bar case: pressure, velocity field and volume fractions of mixture and water phase at different times. Animated version available in Annex 1 to the on-line version of this paper.

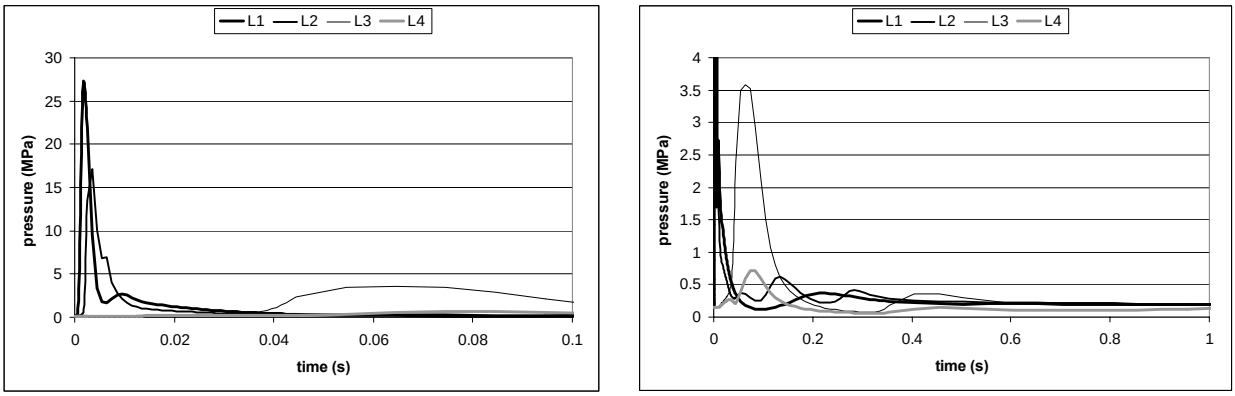

Figure 5 Pressure histories for 400 bar case (left side: initial part of simulation, right side: full simulation). Positions L1-L4 are marked on Figure 3.

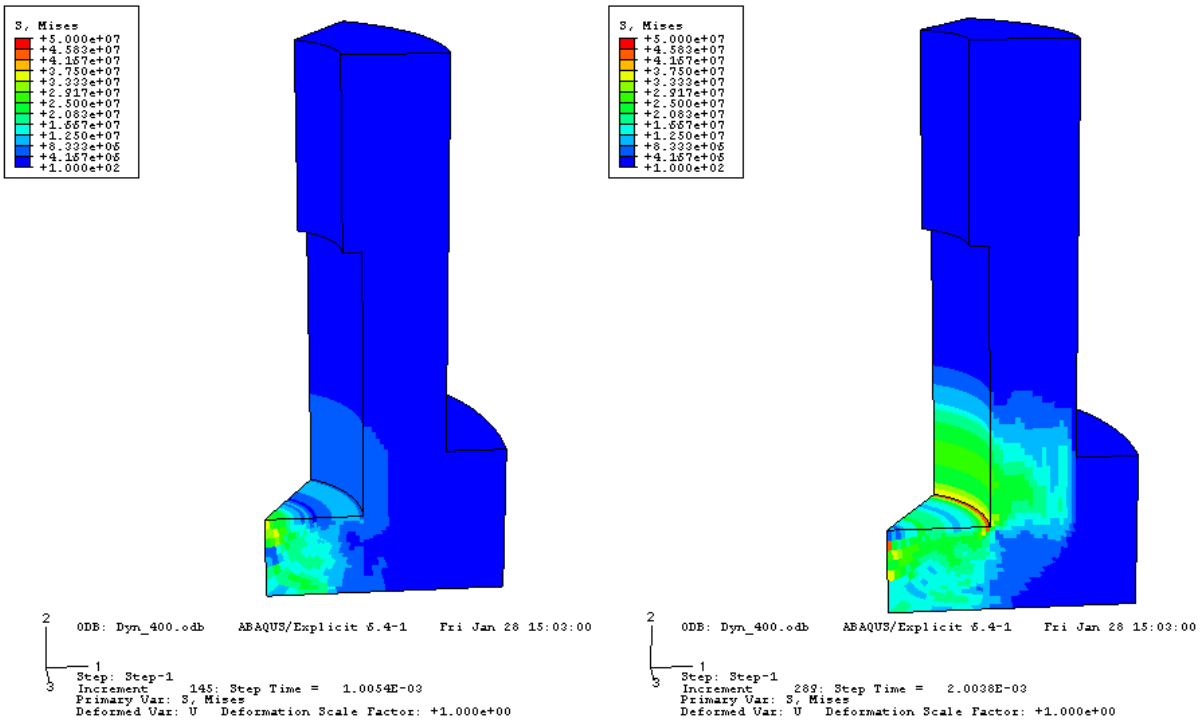

Figure 6 The Mises stresses in the walls of the reactor cavity: 1 and 2 ms, 400 bar

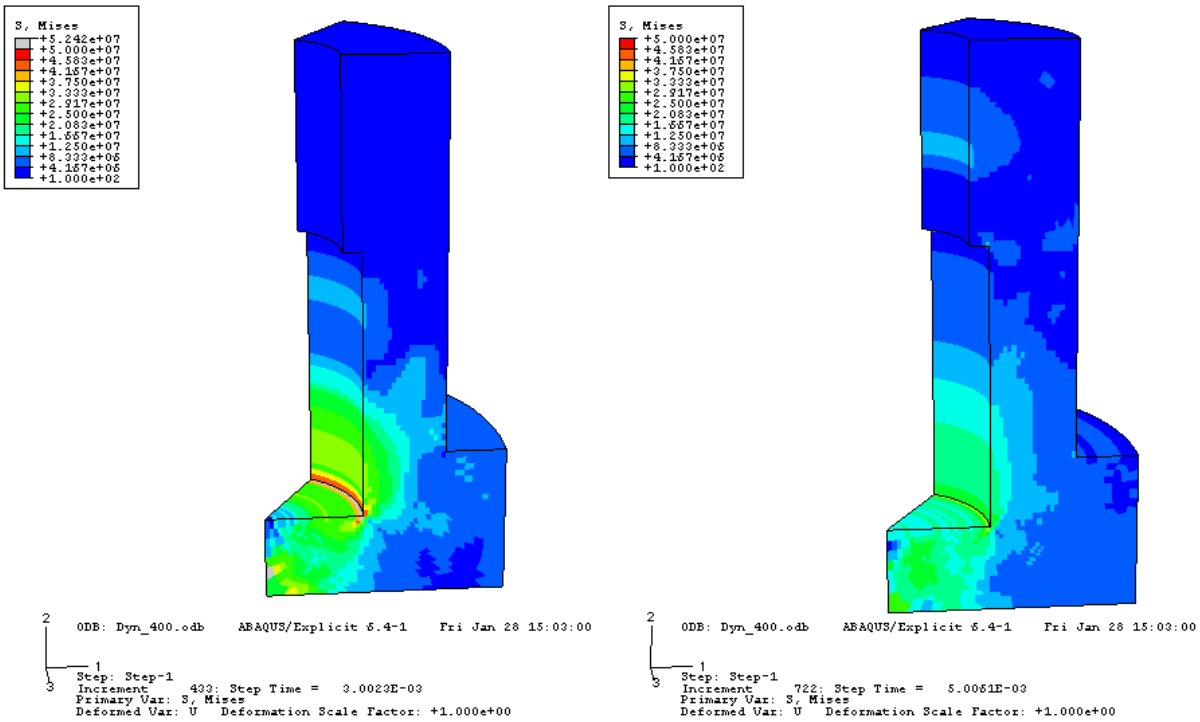

Figure 7 The Mises stresses in the walls of the reactor cavity: 3 and 5 ms, 400 bar

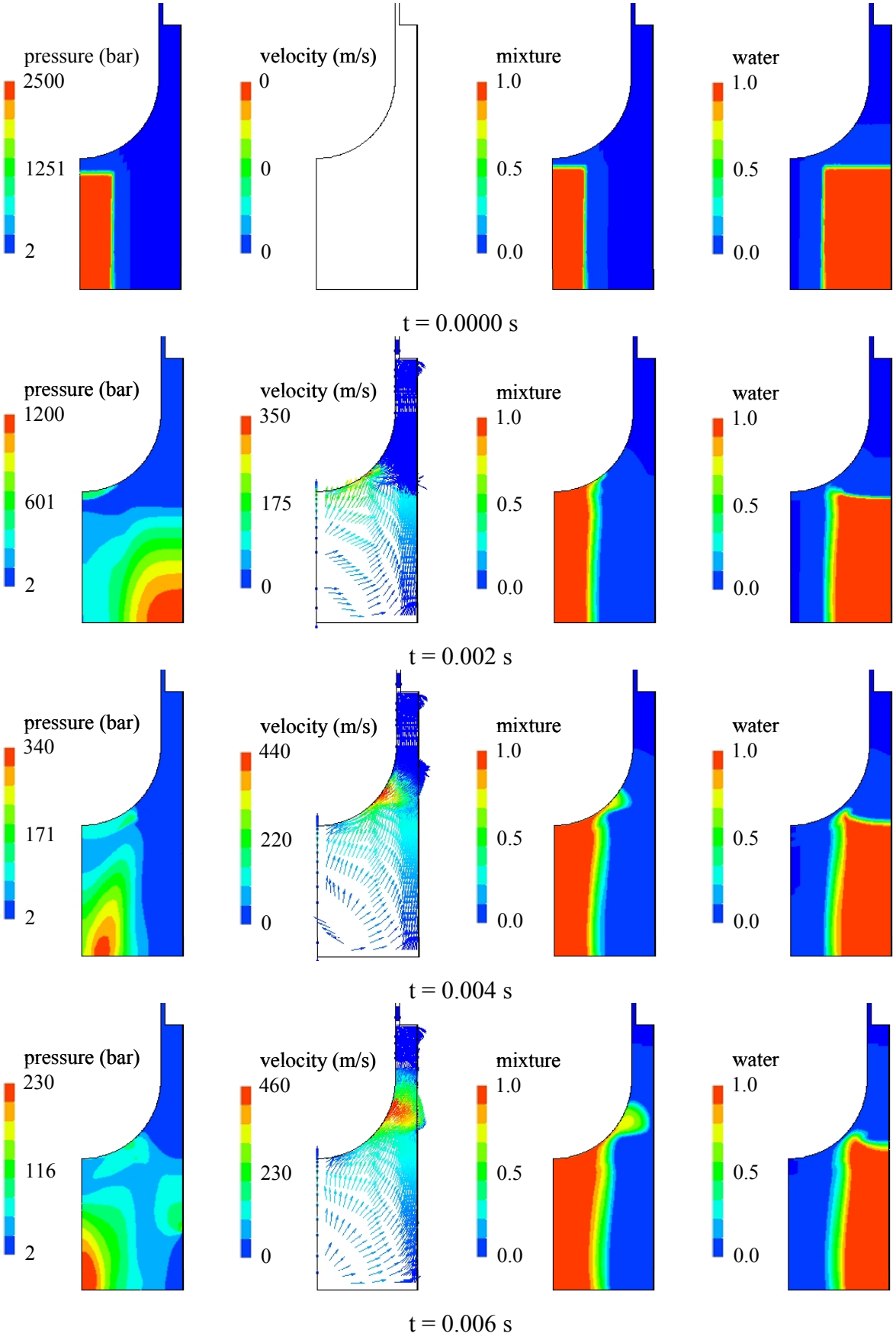

Figure 8 CFD Results for 2500 bar case: pressure, velocity field and volume fractions of mixture and water phase at different times. Animated version available in Annex 3 to the on-line version of this paper.

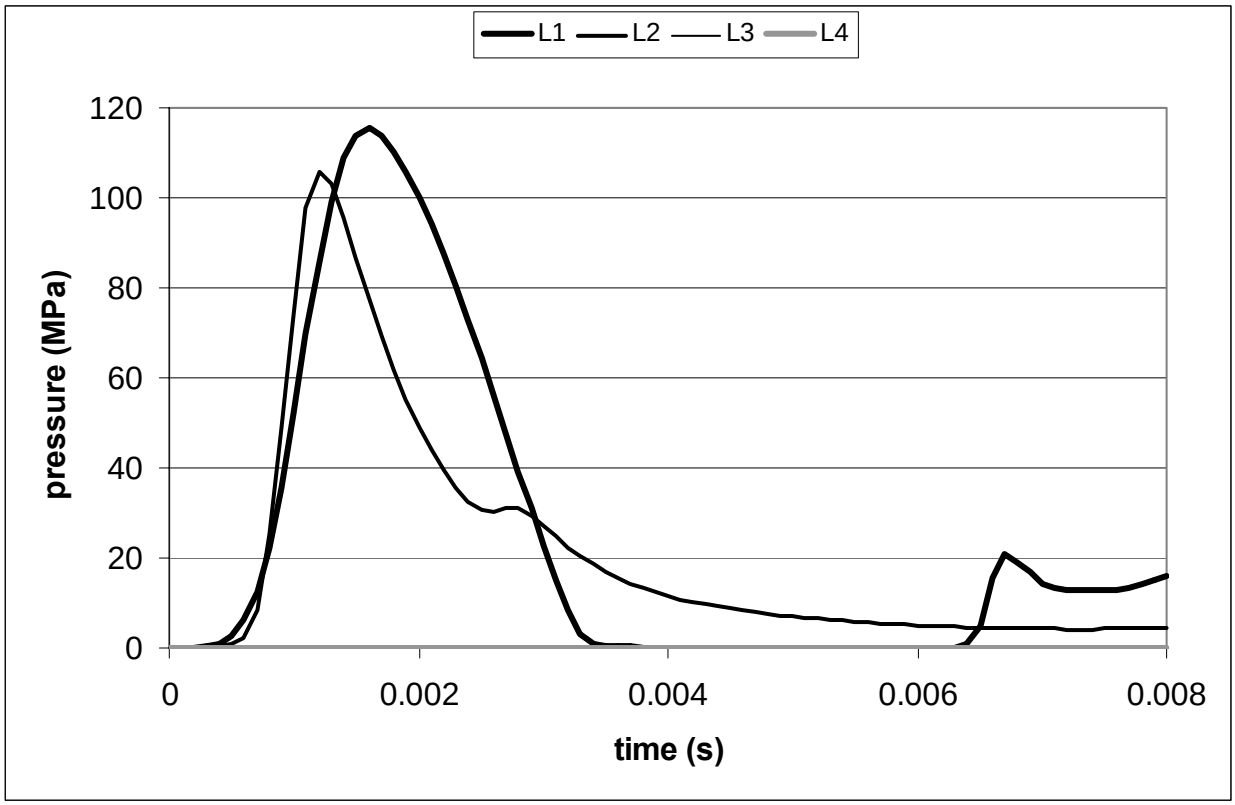

Figure 9 Pressure histories for 2500 bar case. Positions L1-L4 are marked on Figure 3 (pressures at L3 and L4 are too low to be resolved on this diagram).

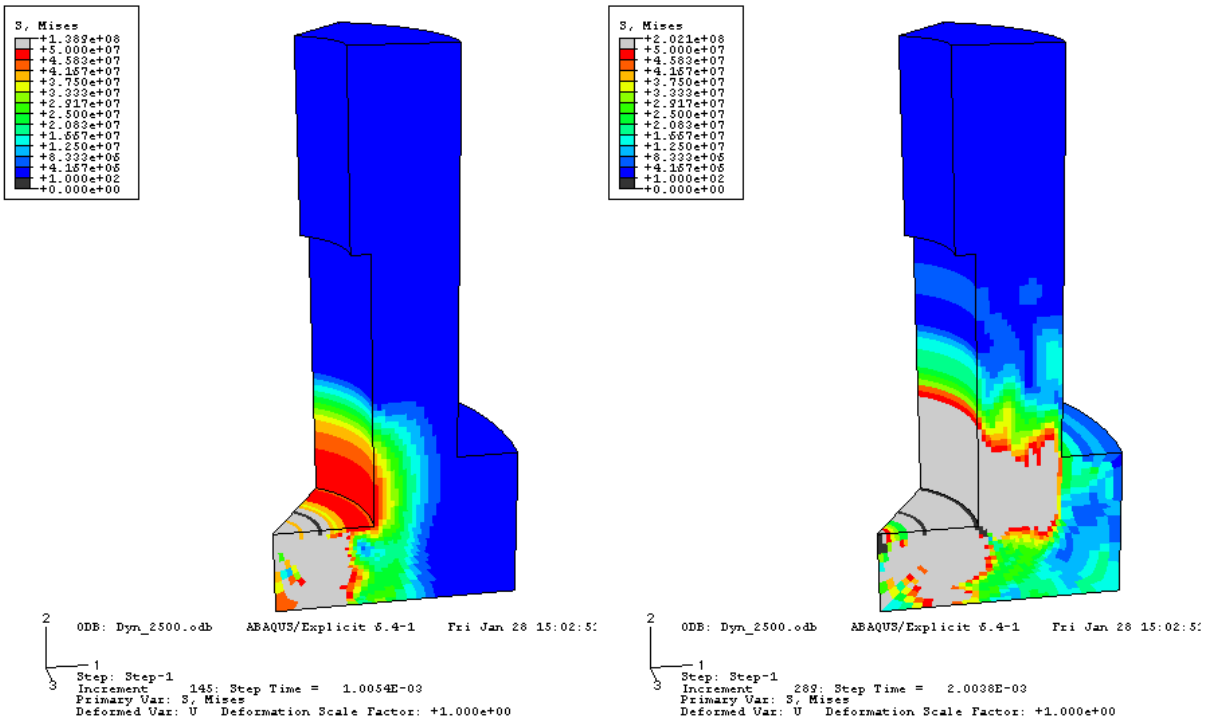

Figure 10 The Mises stresses in the walls of the reactor cavity: 1 and 2 ms, 2500 bar

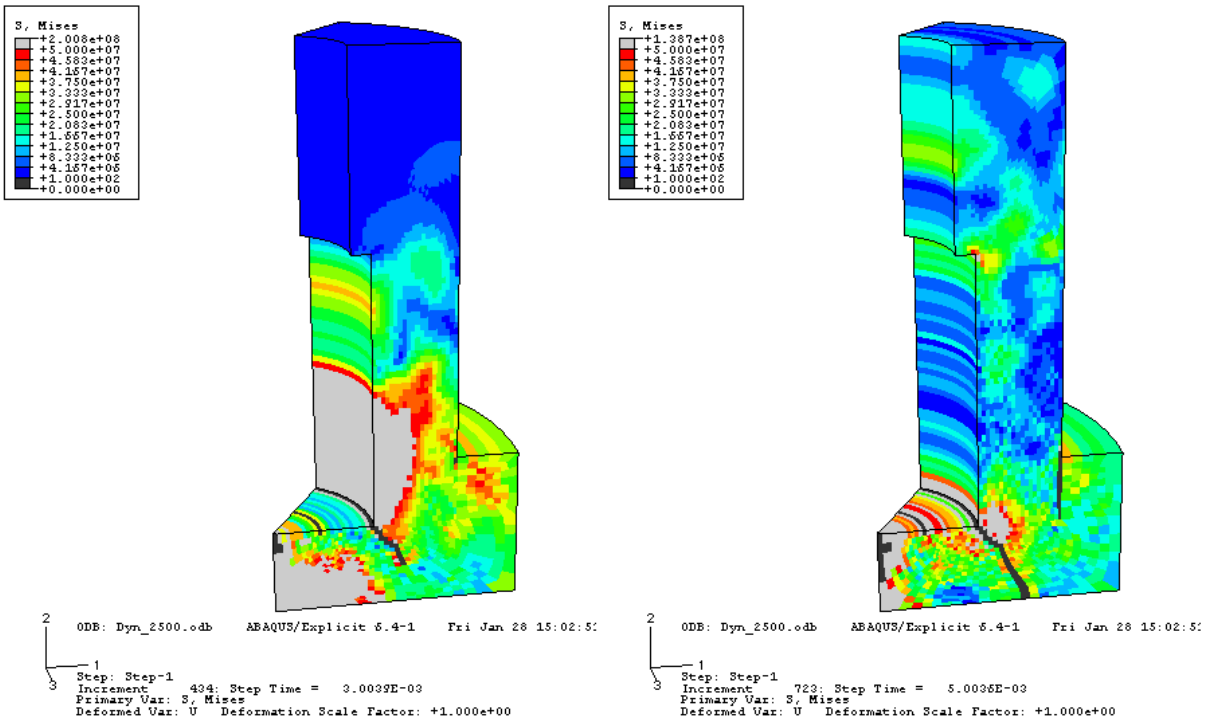

Figure 11 The Mises stresses in the walls of the reactor cavity: 3 and 5 ms; 2500 bar

LIST OF ANIMATIONS

Animation 1 The animated histories of the pressure field, the common velocity field, the mixture volume fraction and the water volume fraction (400 bar).

Animation 2 The animated history of the equivalent Mises stress caused by the dynamic pressure field (400 bar).

Animation 3 The animated histories of the pressure field, the common velocity field, the mixture volume fraction and the water volume fraction (2500 bar).

Animation 4 The animated history of the equivalent Mises stress caused by the dynamic pressure field (2500 bar).

File: fluid_400_bar_NED.mpg

Animation 1 The animated histories of the pressure field, the common velocity field, the mixture volume fraction and the water volume fraction (400 bar).

File: solid_400_bar_NED.avi

Animation 2 The animated history of the equivalent Mises stress caused by the dynamic pressure field (400 bar).

File: fluid_2500_bar_NED.mpg

Animation 3 The animated histories of the pressure field, the common velocity field, the mixture volume fraction and the water volume fraction (2500 bar).

File: solid_2500_bar_NED.avi

Animation 4 The animated history of the equivalent Mises stress caused by the dynamic pressure field (2500 bar).